Eur. J. Mech. A/Solids 20 (2001) 213–226
© 2001 Éditions scientifiques et médicales Elsevier SAS. All rights reserved
S0997-7538(00)01108-6/FLA

Two collinear anti-plane shear cracks in a piezoelectric layer bonded to dissimilar half spaces

Zhen-Gong Zhou, Biao Wang, Mao-Sheng Cao

P.O. Box 1247, Center for Composite Materials, Harbin Institute of Technology, 150001, Harbin, PR China

(Received 16 March 2000; revised 8 June 2000)

Abstract – In this paper, the behaviour of two collinear anti-plane shear cracks in a piezoelectric layer bonded to dissimilar half spaces was investigated by a new method for the impermeable crack face conditions. The cracks are vertical to the interfaces of the piezoelectric layer. By using the Fourier transform, the problem can be solved with two pairs of triple integral equations. These equations are solved using Schmidt's method. This process is quite different from that adopted previously. Numerical examples are provided to show the effect of the geometry of the interacting cracks and the piezoelectric constants of the material upon the stress intensity factor of the cracks. © 2001 Éditions scientifiques et médicales Elsevier SAS

piezoelectric materials / collinear cracks / intensity factors / integral equations

1. Introduction

It is well known that piezoelectric materials produce an electric field when deformed and undergo deformation when subjected to an electric field. The coupling nature of piezoelectric materials has attracted wide applications in electric-mechanical and electric devices, such as electric-mechanical actuators, sensors and structures. When subjected to mechanical and electrical loads in service, these piezoelectric materials can fail prematurely due to defects, e.g. cracks, holes, etc. arising during their manufacturing process. Therefore, it is of great importance to study the electro-elastic interaction and fracture behaviours of piezoelectric materials. Moreover, it is known that the failure of solids results from the cracks, and in most cases, the unstable growth of the crack is brought about by the external loads. So, the study of the fracture mechanics of piezoelectric materials is presently highly relevent.

In the past several years, many studies have been made on the electro-elastic fracture mechanics based on the modelling and analysing of one crack in the piezoelectric materials (see, for examples (Deeg, 1980; Pak, 1990, 1992; Sosa, 1992; Suo et al., 1992; Park and Sun, 1995a, 1995b; Zhang and Tong, 1996; Zhang et al., 1998; Gao et al., 1997; Wang, 1992; Narita and Shindo, 1998a; Shindo et al., 1996; Han et al., 1999)). Narita and Shindo (1998b) investigated the scattering of Love waves by a surface-breaking crack normal to the interface in a piezoelectric layer on an elastic half plane. Li and Mataga (1996a, 1996b) studied the semi-infinite propagating crack in a piezoelectric material with electrode and vacuum boundary conditions on the crack surface under the transient electro-mechanical loads. Chen and Yu (1998), and Meguid and Wang (1998) considered the problem of anti-plane shear wave in an infinite piezoelectric medium under impermeable and permeable crack face conditions, respectively. Chen (1998) obtained the electrically impermeable solution for the infinite piezoelectric strip parallel to the crack under anti-plane shear impact loading. Most recently, Chen and Karihaloo (1999) considered an infinite piezoelectric ceramic with impermeable crack-face boundary condition under arbitrary electro-mechanical impact. Sosa and Khutoryansky (1999) investigated the response of piezoelectric bodies disturbed by internal electric sources. The impermeable boundary condition on the crack surface was widely used in the works (Pak, 1990, 1992; Suo et al., 1992; Suo, 1993; Park and Sun, 1995a, 1995b; Chen and Karihaloo, 1999). In particular, control of laminated structures including piezoelectric devices was the subject of research by Tauchert (1996), Lee and Jiang (1996), Tang et al. (1996), Batra and Liang (1997), and Heyliger (1997). Many piezoelectric devices comprise both piezoelectric and structural layers, and an understanding of the fracture process of piezoelectric structural systems is of great importance in order to ensure the structural integrity of piezoelectric devices (Shindo et al., 1998; Narita and Shindo, 1998b, 1999; Narita et al., 1999). However, the electro-elastic behaviour of laminated piezoelectric composite structures with two cracks has not been studied despite the fact that many piezoelectric devices are constructed in laminated form. Accordingly, there is a need to investigate the electro-elastic fracture mechanics analysis of laminated piezoelectric structures.

In the present paper, we consider the anti-plane shear problem for two cracked piezoelectric layers bonded to two half spaces for the impermeable crack face conditions. The two half spaces have similar properties and the piezoelectric laminate is subjected to combined mechanical and electrical loads. The cracks are situated symmetrically and oriented in the direction vertical to the interfaces of the layer. The interaction between two collinear symmetrical cracks subject to anti-plane shear in piezoelectric layer bonded to two half spaces was investigated using a new method, namely Schmidt's method (Morse et al., 1958). It is a simple and convenient method for solving this problem. A Fourier transform is applied and a mixed boundary value problem is reduced to two pairs of triple integral equations. In solving the triple integral equations, the crack surface displacement and electric potential are expanded in a series using Jacobi's polynomials. This process is quite different from that adopted in references (Han et al., 1999; Deeg, 1980; Pak, 1990, 1992; Sosa, 1992; Suo et al., 1992; Park and Sun, 1995a, 1995b; Zhang and Tong, 1996; Zhang et al., 1998; Gao et al., 1997; Wang, 1992; Narita and Shindo, 1998a, 1999; Shindo et al., 1996; Narita et al., 1999). The form of solution is easy to understand. Numerical calculations are carried out for the stress intensity factors.

2. Formulation of the problem

Consider a piezoelectric layer that is sandwiched between two elastic half planes with an elastic stiffness constant c_{44}^E. Quantities in the half spaces will subsequently be designated by superscript E. The piezoelectric materials layer of thickness $2h$ contains two cracks of length $1-b$ that are vertical to the interfaces, as shown in *Figure 1*. $2b$ is the distance between the cracks (the solution of the piezoelectric layer of width $2h$ containing two collinear Griffith cracks of length $a-b$ can easily be obtained by a simple change in the numerical values of the present paper. $a > b > 0$). The piezoelectric boundary-value problem for anti-plane shear is considerably simplified if we consider only the out-of-plane displacement and the in-plane elastic fields. The plate is subjected to a constant stress $\tau_{yz} = -\tau_0$, and a constant electric displacement $D_y = -D_0$ along the surface of the cracks, such that the constitutive equation can be written as:

$$\tau_{zk} = c_{44} w_{,k} + e_{15} \phi_{,k}, \tag{1}$$

$$D_k = e_{15} w_{,k} - \varepsilon_{11} \phi_{,k}, \tag{2}$$

$$\tau_{xz}^E = c_{44}^E w_{,x}^E, \tag{3}$$

$$\tau_{yz}^E = c_{44}^E w_{,y}^E, \tag{4}$$

where τ_{zk}, D_k $(k = x, y)$ are the anti-plane shear stress and in-plane electric displacement, respectively, $c_{44}, e_{15}, \varepsilon_{11}$ are the shear modulus, piezoelectric coefficient and dielectric parameter, respectively; w and ϕ are the mechanical displacement and electric potential. τ_{xz}^E, τ_{yz}^E and w^E are the shear stress, and the displacement in the half elastic spaces, respectively.

The anti-plane governing equations are (Shindo et al., 1996)

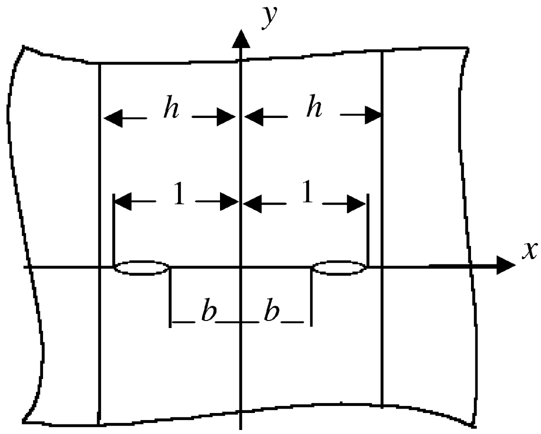

Figure 1. Cracks in a piezoelectric layer body under anti-plane shear.

$$c_{44}\nabla^2 w + e_{15}\nabla^2\phi = 0, \tag{5}$$
$$e_{15}\nabla^2 w - \varepsilon_{11}\nabla^2\phi = 0, \tag{6}$$
$$\nabla^2 w^E = 0, \tag{7}$$

where $\nabla^2 = \partial^2/\partial x^2 + \partial^2/\partial y^2$ is the two-dimensional Laplace operator. Body force, other than inertia, and the free charge are ignored in the present work. Because of the assumed symmetry in geometry and loading, it is sufficient to consider the problem for $0 \leqslant x < \infty$, $0 \leqslant y < \infty$ only.

A Fourier transform is applied to equations (5), (6) and (7). Assume that the solution is:

$$w(x,y) = \frac{2}{\pi}\int_0^\infty A_1(s)\mathrm{e}^{-sy}\cos(sx)\,\mathrm{d}s + \frac{2}{\pi}\int_0^\infty A_2(s)\cosh(sx)\sin(sy)\,\mathrm{d}s, \tag{8}$$

$$w^E(x,y) = \frac{2}{\pi}\int_0^\infty C(s)\mathrm{e}^{-sx}\sin(sy)\,\mathrm{d}s, \tag{9}$$

where $A_1(s)$, $A_2(s)$ and $C(s)$ are unknown functions, and a superposed bar indicates the Fourier transform throughout the paper, e.g.:

$$\overline{f}(s) = \int_{-\infty}^{\infty} f(x)\mathrm{e}^{-isx}\,\mathrm{d}x. \tag{10}$$

Inserting equation (8) into equation (6), it can be assumed:

$$\phi(x,y) - \frac{e_{15}}{\varepsilon_{11}}w(x,y) = \frac{2}{\pi}\int_0^\infty B_1(s)\mathrm{e}^{-sy}\cos(sx)\,\mathrm{d}s + \frac{2}{\pi}\int_0^\infty B_2(s)\cosh(sx)\sin(sy)\,\mathrm{d}s, \tag{11}$$

where $B_1(s)$ and $B_2(s)$ are unknown functions.

As discussion in Narita's (Narita and Shindo, 1999), Shindo's (Shindo et al., 1996) and Yu's (Yu and Chen, 1998) papers, the boundary conditions of the present problem are:

$$\tau_{yz}(x,0) = -\tau_0, \quad b \leqslant |x| \leqslant 1, \tag{12}$$
$$D_y(x,0) = -D_0, \quad b \leqslant |x| \leqslant 1, \tag{13}$$
$$w(x,0) = \phi(x,0) = 0, \quad |x| < b,\ |x| > 1, \tag{14}$$

$$\tau_{xz}(\pm h, y) = \tau_{xz}^E(\pm h, y), \tag{15}$$
$$w(\pm h, y) = w^E(\pm h, y), \tag{16}$$
$$D_x(\pm h, y) = 0, \tag{17}$$
$$w(x, y) = w^E(x, y) = \phi(x, y) = 0, \quad \text{for } \sqrt{x^2 + y^2} \to \infty. \tag{18}$$

The boundary conditions can be applied to yield two pairs of triple integral equations:

$$\frac{2}{\pi}\int_0^\infty A_1(s)\cos(sx)\,\mathrm{d}s = 0, \quad 0 \leqslant x < b, h \geqslant x > 1, \tag{19}$$
$$\frac{2}{\pi}\int_0^\infty sA_1(s)\cos(sx)\,\mathrm{d}s = \frac{2}{\pi}\int_0^\infty sA_2(s)\cosh(sx)\,\mathrm{d}s + \frac{1}{\mu}\left(\tau_0 + \frac{e_{15}D_0}{\varepsilon_{11}}\right), \quad b \leqslant x \leqslant 1, \tag{20}$$

and

$$\frac{2}{\pi}\int_0^\infty B_1(s)\cos(sx)\,\mathrm{d}s = 0, \quad 0 \leqslant x < b, h \geqslant x > 1, \tag{21}$$
$$\frac{2}{\pi}\int_0^\infty sB_1(s)\cos(sx)\,\mathrm{d}s = \frac{2}{\pi}\int_0^\infty sB_2(s)\cosh(sx)\,\mathrm{d}s - \frac{D_0}{\varepsilon_{11}}, \quad b \leqslant x \leqslant 1, \tag{22}$$

where $\mu = c_{44} + \frac{e_{15}^2}{\varepsilon_{11}}$

The relationships between the functions $A_1(s)$, $A_2(s)$, $B_1(s)$, $B_2(s)$ and $C(s)$ are obtained by applying a Fourier sine transform (Gradshteyn and Ryzhik, 1980) to equations (15)–(17):

$$A_2(t)[\sinh(th) + \mu_1\cosh(th)] = \frac{2}{\pi}\int_0^\infty \frac{\sin(sh)s - \tau\mu_1\cos(sh)}{s^2 + t^2}A_1(s)\,\mathrm{d}s, \tag{23}$$
$$C(t)\mathrm{e}^{-th}[\sinh(th) + \mu_1\cosh(th)] = \frac{2}{\pi}\int_0^\infty \frac{\cosh(th)\sin(sh)s + \sinh(th)\cos(sh)t}{s^2 + t^2}A_1(s)\,\mathrm{d}s, \tag{24}$$
$$B_2(t)\sinh(th) = \frac{2}{\pi}\int_0^\infty \frac{s}{s^2 + t^2}B_1(s)\sin(sh)\,\mathrm{d}s, \quad \mu_1 = \frac{c_{44}^E}{\mu}. \tag{25}$$

To determine the unknown functions $A_1(s)$, $B_1(s)$, the above two pairs of triple integral equations (19)–(22) must be solved.

3. Solution of the triple integral equation

The Schmidt's method (Morse et al., 1958) is used to solve the triple integral equations (19)–(22). The displacement w and the electric potential ϕ can be represented by the following series:

$$w(x, 0) = \sum_{n=0}^\infty a_n P_n^{(\frac{1}{2},\frac{1}{2})}\left(\frac{x - \frac{1+b}{2}}{\frac{1-b}{2}}\right)\left(1 - \frac{\left(x - \frac{1+b}{2}\right)^2}{\left(\frac{1-b}{2}\right)^2}\right)^{1/2}, \quad \text{for } b \leqslant x \leqslant 1,\ y = 0, \tag{26}$$
$$w(x, 0) = 0, \quad \text{for } x < b, x > 1, y = 0, \tag{27}$$
$$\phi(x, 0) = \sum_{n=0}^\infty b_n P_n^{(\frac{1}{2},\frac{1}{2})}\left(\frac{x - \frac{1+b}{2}}{\frac{1-b}{2}}\right)\left(1 - \frac{\left(x - \frac{1+b}{2}\right)^2}{\left(\frac{1-b}{2}\right)^2}\right)^{1/2}, \quad \text{for } b \leqslant x \leqslant 1,\ y = 0, \tag{28}$$
$$\phi(x, 0) = 0, \quad \text{for } x < b, x > 1, y = 0, \tag{29}$$

where a_n and b_n are unknown coefficients to be determined and $P_n^{(1/2,1/2)}(x)$ is a Jacobi polynomial (Gradshteyn and Ryzhik, 1980). The Fourier transformation of equations (26) and (28) is (Erdelyi, 1954):

$$A_1(s) = \overline{w}(s,0) = \sum_{n=0}^{\infty} a_n Q_n G_n(s) \frac{1}{s} J_{n+1}\left(s\frac{1-b}{2}\right), \tag{30}$$

$$B_1(s) = \overline{\phi}(s,0) - \frac{e_{15}}{\varepsilon_{11}}\overline{w}(s,0) = \sum_{n=0}^{\infty}\left(b_n - \frac{e_{15}}{\varepsilon_{11}}a_n\right) Q_n G_n(s)\frac{1}{s} J_{n+1}\left(s\frac{1-b}{2}\right), \tag{31}$$

$$Q_n = 2\sqrt{\pi}\frac{\Gamma\left(n+1+\frac{1}{2}\right)}{n!}, \tag{32}$$

$$G_n(s) = \begin{cases} (-1)^{\frac{n}{2}} \cos\left(s\dfrac{1+b}{2}\right), & n = 0, 2, 4, 6, \ldots, \\ (-1)^{\frac{n-1}{2}} \sin\left(s\dfrac{1+b}{2}\right), & n = 1, 3, 5, 7, \ldots, \end{cases} \tag{33}$$

where $\Gamma(x)$ and $J_n(x)$ are the Gamma and Bessel functions, respectively.

Substituting equations (30) and (31), respectively, into equations (19)–(22), satisfies equations (19) and (21). After integration with respect to x in $[b, x]$, equations (20) and (22) reduce to the form, respectively.

$$\begin{aligned} &\sum_{n=0}^{\infty} a_n Q_n \int_0^{\infty} s^{-1} G_n(s) J_{n+1}\left(s\frac{1-b}{2}\right)[\sin(sx) - \sin(sb)]\,\mathrm{d}s \\ &\quad = \frac{\pi}{2\mu}\tau_0(1+\lambda)(x-b) + \frac{2}{\pi}\sum_{n=0}^{\infty} a_n Q_n \int_0^{\infty} \frac{\sinh(sx) - \sinh(sb)}{\sinh(sh) + \mu_1\cosh(sh)}\,\mathrm{d}s \\ &\qquad \times \int_0^{\infty} G_n(\eta) J_{n+1}\left(\eta\frac{1-b}{2}\right)\frac{\eta\sin(\eta h) - s\mu_1\cos(\eta h)}{(\eta^2+s^2)\eta}\,\mathrm{d}\eta, \end{aligned} \tag{34}$$

$$\begin{aligned} &\sum_{n=0}^{\infty}\left(b_n - \frac{e_{15}}{\varepsilon_{11}}a_n\right) Q_n \int_0^{\infty} s^{-1} G_n(s) J_{n+1}\left(s\frac{1-b}{2}\right)[\sin(sx) - \sin(sb)]\,\mathrm{d}s \\ &\quad = -\frac{\pi D_0}{2\varepsilon_{11}}(x-b) \\ &\qquad + \frac{2}{\pi}\sum_{n=0}^{\infty}\left(b_n - \frac{e_{15}}{\varepsilon_{11}}a_n\right) Q_n \int_0^{\infty}\frac{\sinh(sx) - \sinh(sb)}{\sinh(sh)}\,\mathrm{d}s\int_0^{\infty} G_n(\eta) J_{n+1}\left(\eta\frac{1-b}{2}\right)\frac{\sin(\eta h)}{(\eta^2+s^2)}\,\mathrm{d}\eta, \end{aligned} \tag{35}$$

where $\lambda = \frac{e_{15}D_0}{\varepsilon_{11}\tau_0}$.

For a large s, the integrands of the double semi-infinite integral in equations (34) and (35) almost all have exponential forms, so the double semi-infinite integral can be evaluated numerically by Filon's method (Amemiya and Taguchi, 1969). The semi-infinite integral in equations (34) and (35) is modified as (Gradshteyn and Ryzhik, 1980):

$$\begin{aligned} &\int_0^{\infty}\frac{1}{s}J_{n+1}\left(s\frac{1-b}{2}\right)\cos\left(s\frac{1+b}{2}\right)\sin(sx)\,\mathrm{d}s \\ &\quad = \frac{1}{2(n+1)}\left\{\frac{\left(\frac{1-b}{2}\right)^{n+1}\sin\left(\frac{(n+1)\pi}{2}\right)}{\left\{x+\frac{1+b}{2}+\sqrt{\left(x+\frac{1+b}{2}\right)^2 - \left(\frac{1-b}{2}\right)^2}\right\}^{n+1}} - \sin\left[(n+1)\sin^{-1}\left(\frac{1+b-2x}{1-b}\right)\right]\right\}, \end{aligned} \tag{36}$$

$$\int_0^\infty \frac{1}{s} J_{n+1}\left(s\frac{1-b}{2}\right)\sin\left(s\frac{1+b}{2}\right)\sin(sx)\,\mathrm{d}s$$
$$= \frac{1}{2(n+1)}\left\{\cos\left[(n+1)\sin^{-1}\left(\frac{1+b-2x}{1-b}\right)\right] - \frac{\left(\frac{1-b}{2}\right)^{n+1}\cos\left(\frac{(n+1)\pi}{2}\right)}{\left\{x+\frac{1+b}{2}+\sqrt{\left(x+\frac{1+b}{2}\right)^2-\left(\frac{1-b}{2}\right)^2}\right\}^{n+1}}\right\}. \quad (37)$$

Thus the semi-infinite integral can be evaluated directly. Equations (34) and (35) can now be solved for the coefficients a_n and b_y by the Schmidt's method (Morse et al., 1958). For brevity, equation (34) can be rewritten as (equation (35) can be solved using similar method as following):

$$\sum_{n=0}^{\infty} a_n E_n(x) = U(x), \quad b < x < 1, \quad (38)$$

where $E_n(x)$ and $U(x)$ are known functions. Coefficients a_n are unknown and will be determined. A set of functions $P_n(x)$ which satisfy the orthogonality condition:

$$\int_b^1 P_m(x)P_n(x)\,\mathrm{d}x = N_n\delta_{mn}, \quad N_n = \int_b^1 P_n^2(x)\,\mathrm{d}x, \quad (39)$$

can be constructed from the function, $E_n(x)$, such that:

$$P_n(x) = \sum_{i=0}^{n} \frac{M_{in}}{M_{nn}} E_i(x), \quad (40)$$

where M_{in} is the cofactor of the element d_{in} of D_n, which is defined as:

$$D_n = \begin{bmatrix} d_{00}, & d_{01}, & d_{02}, & \ldots, & d_{0n} \\ d_{10}, & d_{11}, & d_{12}, & \ldots, & d_{1n} \\ d_{20}, & d_{21}, & d_{22}, & \ldots, & d_{2n} \\ \cdots & \cdots & \cdots & \cdots & \cdots \\ \cdots & \cdots & \cdots & \cdots & \cdots \\ \cdots & \cdots & \cdots & \cdots & \cdots \\ d_{n0}, & d_{n1}, & d_{n2}, & \ldots, & d_{nn} \end{bmatrix}, \quad d_{ij} = \int_b^1 E_i(x)E_j(x)\,\mathrm{d}x. \quad (41)$$

Using equations (38) $\sim$ (41), we obtain:

$$a_n = \sum_{j=n}^{\infty} q_j \frac{M_{nj}}{M_{jj}} \quad (42)$$

with

$$q_j = \frac{1}{N_j}\int_b^1 U(x)P_j(x)\,\mathrm{d}x. \quad (43)$$

4. Intensity factors

Although we can determine the entire stress field and the electric displacement from coefficients a_n and b_n. It is of importance in fracture mechanics to determine stress τ_{yz} and the electric displacement D_y in the vicinity of the cracks' tips. τ_{yz} and D_y along the crack line can be expressed respectively as:

$$\begin{aligned}\tau_{yz}(x,0) = &-\frac{2\mu}{\pi}\sum_{n=0}^{\infty} a_n Q_n \left[\int_0^\infty G_n(s) J_{n+1}\left(s\frac{1-b}{2}\right)\cos(xs)\,\mathrm{d}s\right. \\ &\left.-\frac{2}{\pi}\int_0^\infty \frac{\cosh(sx)s}{\sinh(sh)+\mu_1\cosh(sh)}\,\mathrm{d}s \int_0^\infty G_n(\eta) J_{n+1}\left(\eta\frac{1-b}{2}\right)\frac{\eta\sin(\eta h)-s\mu_1\cos(\eta h)}{(\eta^2+s^2)\eta}\,\mathrm{d}\eta\right] \\ &-\frac{2e_{15}}{\pi}\sum_{n=0}^{\infty}\left(b_n-\frac{e_{15}}{\varepsilon_{11}}a_n\right) Q_n \left[\int_0^\infty G_n(s) J_{n+1}\left(s\frac{1-b}{2}\right)\cos(xs)\,\mathrm{d}s\right. \\ &\left.-\frac{2}{\pi}\int_0^\infty \frac{\cosh(sx)s}{\sinh(sh)}\,\mathrm{d}s \int_0^\infty G_n(\eta) J_{n+1}\left(\eta\frac{1-b}{2}\right)\frac{\sin(\eta h)}{(\eta^2+s^2)}\,\mathrm{d}\eta\right],\end{aligned} \tag{44}$$

$$\begin{aligned}D_y(x,0) = &\frac{2}{\pi}\sum_{n=0}^{\infty}(\varepsilon_{11}b_n - e_{15}a_n) Q_n \left[\int_0^\infty G_n(s) J_{n+1}\left(s\frac{1-b}{2}\right)\cos(xs)\,\mathrm{d}s\right. \\ &\left.-\frac{2}{\pi}\int_0^\infty \frac{\cosh(sx)s}{\sinh(sh)}\,\mathrm{d}s \int_0^\infty G_n(\eta) J_{n+1}\left(\eta\frac{1-b}{2}\right)\frac{\sin(\eta h)}{(\eta^2+s^2)}\,\mathrm{d}\eta\right].\end{aligned} \tag{45}$$

Observing the expression in equations (44) and (45), the singular portion of the stress field and the singular portion of electric displacement can be obtained respectively from the relationships (Gradshteyn and Ryzhik, 1980):

$$\cos\left(s\frac{1+b}{2}\right)\cos(sx) = \frac{1}{2}\left\{\cos\left[s\left(\frac{1+b}{2}-x\right)\right]+\cos\left[s\left(\frac{1+b}{2}+x\right)\right]\right\},$$

$$\sin\left(s\frac{1+b}{2}\right)\cos(sx) = \frac{1}{2}\left\{\sin\left[s\left(\frac{1+b}{2}-x\right)\right]+\sin\left[s\left(\frac{1+b}{2}+x\right)\right]\right\},$$

$$\int_0^\infty J_n(sa)\cos(bs)\,\mathrm{d}s = \begin{cases} \dfrac{\cos[n\sin^{-1}(b/a)]}{\sqrt{a^2-b^2}}, & a>b, \\ -\dfrac{a^n\sin(n\pi/2)}{\sqrt{b^2-a^2}[b+\sqrt{b^2-a^2}]^n}, & b>a, \end{cases}$$

$$\int_0^\infty J_n(sa)\sin(bs)\,\mathrm{d}s = \begin{cases} \dfrac{\sin[n\sin^{-1}(b/a)]}{\sqrt{a^2-b^2}}, & a>b, \\ \dfrac{a^n\cos(n\pi/2)}{\sqrt{b^2-a^2}[b+\sqrt{b^2-a^2}]^n}, & b>a. \end{cases}$$

The singular portion of the stress field and the singular portion of electric displacement can be expressed respectively as follows:

$$\tau = -\frac{1}{\pi}\sum_{n=0}^{\infty}(c_{44}a_n + e_{15}b_n) Q_n H_n(b,x), \tag{46}$$

$$D = \frac{1}{\pi}\sum_{n=0}^{\infty}(\varepsilon_{11}b_n - e_{15}a_n) Q_n H_n(b,x), \tag{47}$$

where

$$H_n(b,x) = -F_1(b,x,n), \quad n = 0,1,2,3,4,5,\dots \text{ (for } 0 < x < b),$$
$$H_n(b,x) = (-1)^{n+1} F_2(b,x,n), \quad n = 0,1,2,3,4,5,\dots \text{ (for } 1 < x),$$
$$F_1(b,x,n) = \frac{2(1-b)^{n+1}}{\sqrt{(1+b-2x)^2-(1-b)^2}[1+b-2x+\sqrt{(1+b-2x)^2-(1-b)^2}]^{n+1}},$$
$$F_2(b,x,n) = \frac{2(1-b)^{n+1}}{\sqrt{(2x-1-b)^2-(1-b)^2}[2x-1-b+\sqrt{(2x-1-b)^2-(1-b)^2}]^{n+1}}.$$

At the left tip of the right crack, we obtain the stress intensity factor K_L as:

$$K_L = \lim_{x\to b^-} \sqrt{2\pi(b-x)} \cdot \tau = \sqrt{\frac{2}{\pi(1-b)}} \sum_{n=0}^{\infty} (c_{44}a_n + e_{15}b_n) Q_n. \tag{48}$$

At the right tip of the right crack, we obtain the stress intensity factor K_R as:

$$K_R = \lim_{x\to 1^+} \sqrt{2\pi(x-1)} \cdot \tau = \sqrt{\frac{2}{\pi(1-b)}} \sum_{n=0}^{\infty} (-1)^n (c_{44}a_n + e_{15}b_n) Q_n. \tag{49}$$

At the left tip of the right crack, we obtain the electric displacement intensity factor K_L^D as:

$$K_L^D = \lim_{x\to b^-} \sqrt{2\pi(b-x)} \cdot D = \sqrt{\frac{2}{\pi(1-b)}} \sum_{n=0}^{\infty} (e_{15}a_n - \varepsilon_{11}b_n) Q_n. \tag{50}$$

At the right tip of the right crack, we obtain the electric displacement intensity factor K_R^D as:

$$K_R^D = \lim_{x\to 1^+} \sqrt{2\pi(x-1)} \cdot D = \sqrt{\frac{2}{\pi(1-b)}} \sum_{n=0}^{\infty} (-1)^n (e_{15}a_n - \varepsilon_{11}b_n) Q_n. \tag{51}$$

5. Numerical calculations and discussion

This section presents numerical results of several representative problems. Adopting the first ten terms of the infinite series to equation (38), we performed the Schmidt procedure. For a check of the accuracy, the values

Table I. Values of $\sum_0^9 a_n E_n(x)/(\frac{\pi\tau_0(1+\lambda)}{2\mu})$ and $U(x)/(\frac{\pi\tau_0(1+\lambda)}{2\mu}) = x - b$ for $b = 0.1$, $h = 1.1$, $\lambda = 0.2$ (aluminum/PZT-4/aluminum).

x	$\sum_0^9 a_n E_n(x)/(\frac{\pi\tau_0(1+\lambda)}{2\mu})$	$U(x)/(\frac{\pi\tau_0(1+\lambda)}{2\mu}) = x - b$
0.1	0.0000	0.0000
0.2	0.10069	0.1000
0.3	0.20058	0.2000
0.4	0.30002	0.3000
0.5	0.39987	0.4000
0.6	0.49925	0.5000
0.7	0.59992	0.6000
0.8	0.70008	0.7000
0.9	0.80006	0.8000

of $\sum_0^9 a_n E_n(x)$ and $U(x)$ are given in *table I* for $b = 0.1$, $h = 1.1$, $\lambda = 0.2$ (aluminum/PZT-4/aluminum). In *table II*, the values of the coefficients a_n are given for $b = 0.1$, $h = 1.1$, $\lambda = 0.2$ (aluminum/PZT-4/aluminum). From the above results and references (see, e.g., Itou, 1978, 1979, Zhou, 1999a, 1999b), it can be seen that the Schmidt's method is performed satisfactorily if the first ten terms of the infinite series to equation (38) are obtained. The behaviour of the solution stays steady with an increase of the number of terms in equation (38). Hence, it is clear that the Schmidt's method is carried out satisfactorily. The precision of the present paper's solution can satisfy the demands of the practical problem. The solution of two collinear cracks of arbitrary length $a - b$ can easily be obtained by a simple change in the numerical values of the present paper ($a > b > 0$),

Table II. Values of $a_n/(\frac{\pi\tau_0(1+\lambda)}{2\mu})$ for $b = 0.1$, $h = 1.1$, $\lambda = 0.2$ (aluminum/PZT-4/aluminum).

n	$a_n/(\frac{\pi\tau_0(1+\lambda)}{2\mu})$
0	0.353514E+00
1	0.753116E–02
2	0.781870E–03
3	0.484239E–04
4	0.992569E–06
5	0.245309E–07
6	0.743541E–08
7	0.563344E–09
8	0.693542E–10
9	0.745892E–11

Table III. Material properties used in the examples.

	Piezoelectric layer			Elastic half plane	
	PZT-4	PZT-5H		Aluminum	Epoxy
c_{44} $(\times 10^{10}\ \mathrm{N/m^2})$	2.56	2.3	c_{44}^E	2.65	0.176
e_{15} $(\mathrm{c/m^2})$	12.7	17.0		0	0
ε_{11} $(\times 10^{-10}\ \mathrm{c/Vm^2})$	64.6	150.4		–	–

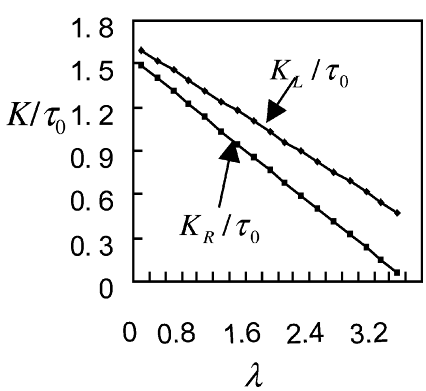

Figure 2. Stress intensity factors versus λ for $b = 0.1$, $h = 1.1$ (aluminum/PZT-4/aluminum).

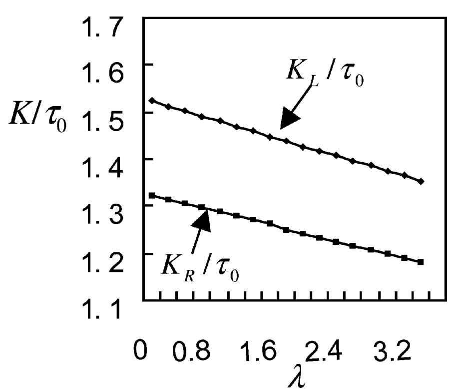

Figure 3. Stress intensity factors versus λ for $b = 0.1$, $h = 2.0$ (aluminum/PZT-4/aluminum).

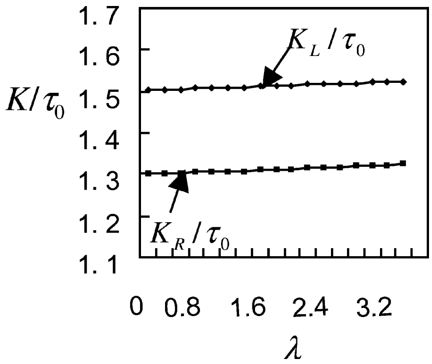

Figure 4. Stress intensity factors versus λ for $b = 0.1$, $h = 4.0$ (aluminum/PZT-4/aluminum).

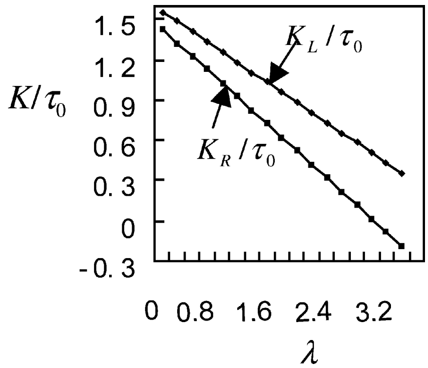

Figure 5. Stress intensity factors versus λ for $b = 0.1$, $h = 1.1$ (aluminum/PZT-4/aluminum).

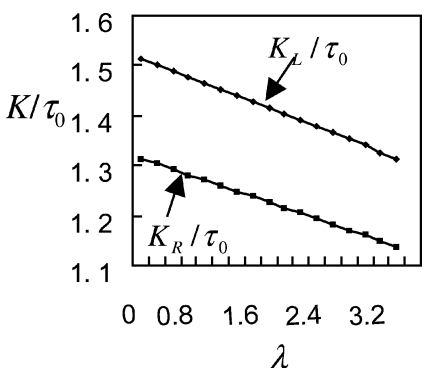

Figure 6. Stress intensity factors versus λ for $b = 0.1$, $h = 2.0$ (aluminum/PZT-5H/aluminum).

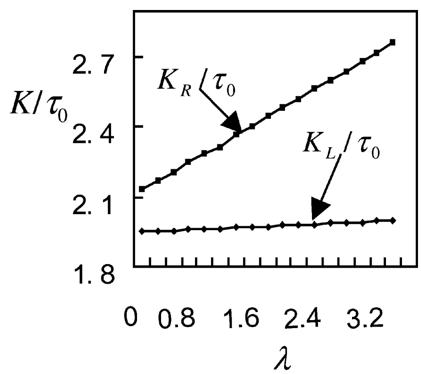

Figure 7. Stress intensity factors versus λ for $b = 0.1$, $h = 1.1$ (epoxy/PZT-5H/epoxy).

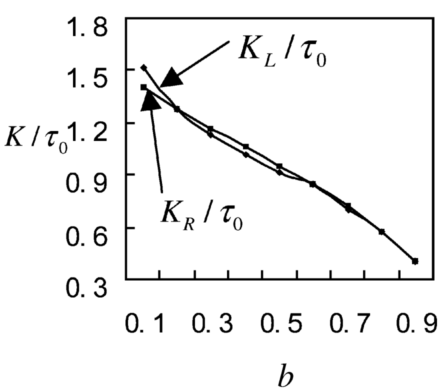

Figure 8. Stress intensity factors versus b for $\lambda = 0.2$, $h = 1.1$ (aluminum/PZT-4/aluminum).

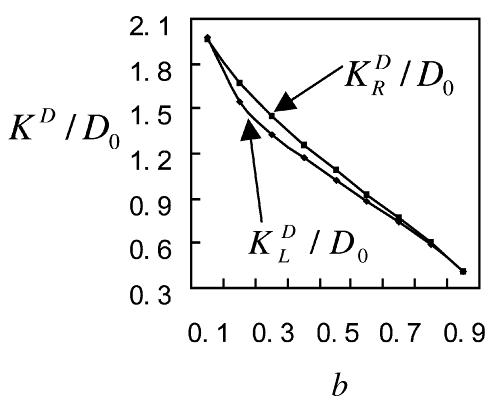

Figure 9. Electric intensity factors versus b for $\lambda = 0.2$, $h = 1.1$ (aluminum/PZT-4/aluminum).

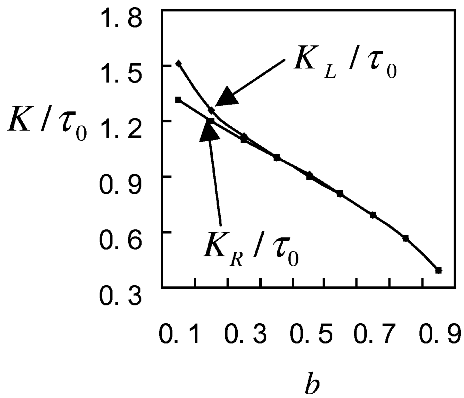

Figure 10. Stress intensity factors versus b for $\lambda = 0.2$, $h = 2.0$ (aluminum/PZT-4/aluminum).

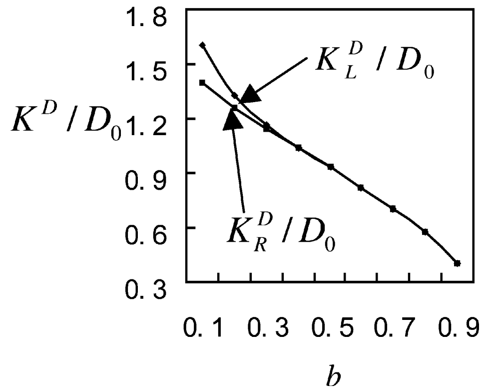

Figure 11. Electric intensity factors versus b for $\lambda = 0.2$, $h = 2.0$ (aluminum/PZT-4/aluminum).

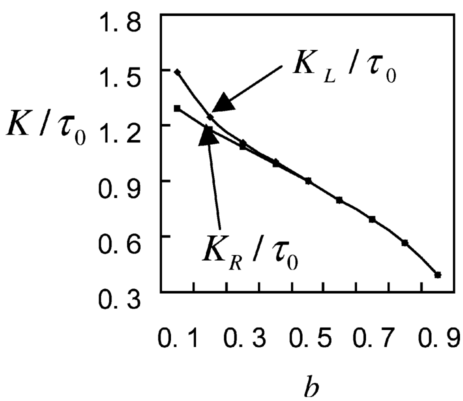

Figure 12. Stress intensity factors versus b for $\lambda = 0.2$, $h = 5.0$ (aluminum/PZT-4/aluminum).

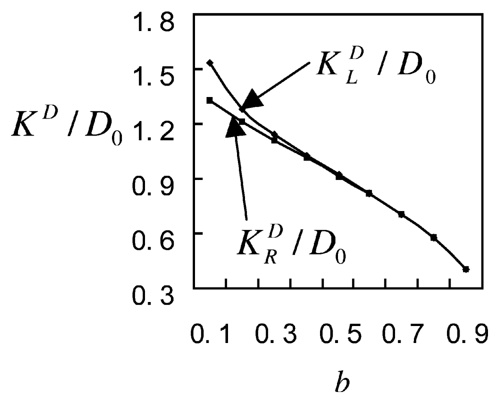

Figure 13. Electric intensity factors versus b for $\lambda = 0.2$, $h = 5.0$ (aluminum/PZT-4/aluminum).

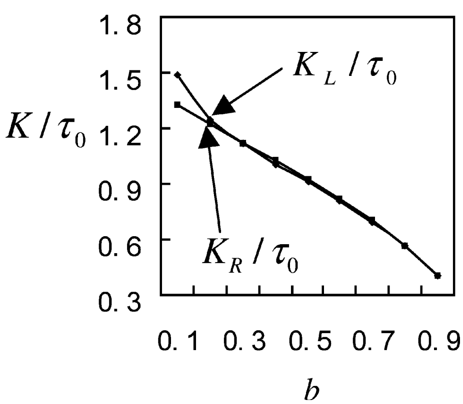

Figure 14. Stress intensity factors versus b for $\lambda = 0.2$, $h = 1.1$ (aluminum/PZT-5H/aluminum).

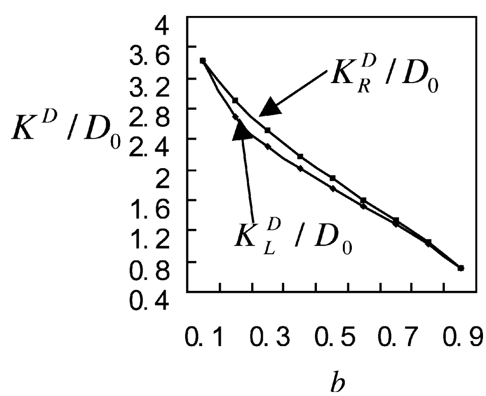

Figure 15. Electric intensity factors versus b for $\lambda = 0.2$, $h = 1.1$ (aluminum/PZT-5H/aluminum).

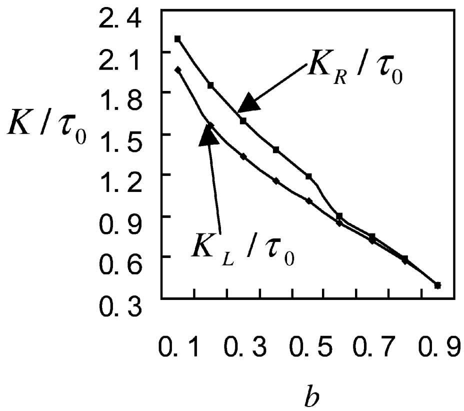

Figure 16. Stress intensity factors versus b for $\lambda = 0.2$, $h = 1.1$ (epoxy/PZT-4/epoxy).

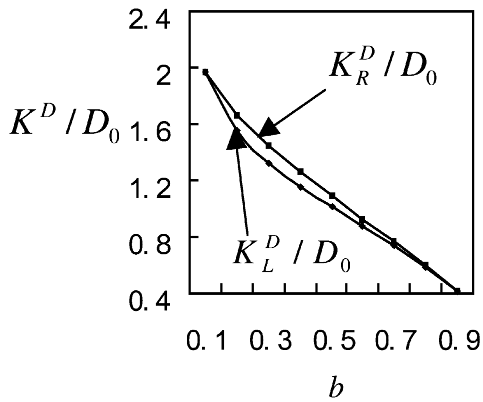

Figure 17. Electric intensity factors versus b for $\lambda = 0.2$, $h = 1.1$ (epoxy/PZT-4/epoxy).

i.e., it can use the results of the collinear cracks of length $1 - b/a$ and the strip width h/a in the present paper. The solution of this paper is suitable for the arbitrary length two collinear cracks in the piezoelectric layers bonded to dissimilar half spaces. All applications were focused on two cracked piezoelectric layer bonded to half planes. The piezoelectric layers is assumed to be the commercially available piezoelectric PZT-4 or PZT-5H, and the half planes are either aluminum or epoxy. The engineering material constants are listed in *table III* (Narita et al., 1999). The results of the present paper are shown in *figures 2–17*, respectively. From the results, the following observations are very significant:

(i) The stress intensity factors not only depend on the crack length, the electric loading and the width of the piezoelectric layer, but also depend on the properties of the materials.

(ii) The effects of the two collinear cracks decrease when the distance between the two collinear cracks increases.

(iii) The electric displacement intensity factors decrease when the width of the piezoelectric layer increases.

(iv) The solutions of this paper are close to ones of two collinear Griffith cracks in infinite piezoelectric materials for width $h \geqslant 5.0$, that is the influence of the width of the piezoelectric layer to the results is small for the case $h \geqslant 5.0$.

(v) The influence of the electric loading to the results is large for a thin piezoelectric layer. However, the influence of the electric loading to the results is very small for the thick piezoelectric layer. This is consistent with the conclusion that the stress intensity factor is independent of the electric loading for infinite piezoelectric materials.

(vi) The stress and electric displacement intensity factors at the inner crack tips are smaller or larger than ones at the outer crack tips for the thin piezoelectric layer. This kind of phenomenon is induced by the coupling of the mechanical and electric, and by the width of the piezoelectric layer and the crack interaction, such as in *figures 8, 9* and *14–17*, respectively. However, for $h \geqslant 5.0$, the stress and electric displacement intensity factors at the inner crack tips are larger than ones at the outer crack tips.

(vii) The stress intensity factor becomes small or large with the increasing of the electric loading for the different material composition cases. It can be concluded that the electric field will reduce or increase the magnitude of the stress intensity factor for the different material composition cases. This is due to the coupling between the electric and the mechanical fields.

6. Conclusions

We have developed an electro-elastic fracture mechanics theory to determine the singular stress and electric fields near the crack tip for piezoelectric laminates having two finite cracks normal to the interface under longitudinal shear. The anti-plane electro-elastic problem of a piezoelectric layer with two collinear cracks has been analysed theoretically. The traditional concept of linear elastic fracture mechanics is extended to include the piezoelectric effects and the results are expressed in terms of the stress intensity factors. The stress and electric displacement intensity factors of the cracked piezoelectric laminates were computed, and the results were presented to study the influence of the electrical fields on the fracture behaviour of the piezoelectric laminates. The stress intensity factor can either be increased or decreased by varying the piezoelectric and elastic material properties. It is possible to adjust these material and geometric parameters in order to reduce the magnitude of the stress intensity factors.

Acknowledgements

The authors are grateful for financial support from the Post Doctoral Science Foundation of Hei Long Jiang Province, the Natural Science Foundation of Hei Long Jiang Province and The National Foundation for Excellent Young Investigations.

References

Amemiya A., Taguchi T., 1969. Numerical Analysis and Fortran, Maruzen, Tokyo.

Batra R.C., Liang X.Q., 1997. The vibration of a rectangular laminated elastic plate with embedded piezoelectric sensors and actuators. Computer and Structures 63, 203.

Chen Z.T., 1998. Crack tip field of an infinite piezoelectric strip under anti-plane impact. Mechanics Research Communications 25, 313–319.

Chen Z.T., Karihaloo B.L., 1999. Dynamic response of a cracked piezoelectric ceramic under arbitrary electro-mechanical impact. International Journal of Solids and Structures 36, 5125–5133.

Chen Z.T., Yu S.W., 1998. Anti-plane dynamic fracture mechanics in piezoelectric materials. International Journal of Fracture 85, L3–L12.

Deeg W.E.F., 1980. The analysis of dislocation, crack and inclusion problems in piezoelectric solids, PhD thesis, Stanford University.

Dunn M.L., 1994. The effects of crack face boundary conditions on the fracture mechanics of piezoelectric solids. Engineering Fracture Mechanics 48, 25–39.

Erdelyi A. (Ed.), 1954. Tables of Integral Transforms, Vol.1, McGraw-Hill, New York.

Gao H., Zhang T.Y., Tong P., 1997. Local and global energy rates for an elastically yielded crack in piezoelectric ceramics. Journal of Mechanics and Physics of Solids 45, 491–510.

Gradshteyn I.S., Ryzhik I.M., 1980. Table of Integral, Series and Products, Academic Press, New York.

Han Xue-Li, Wang Tzuchiang, 1999. Interacting multiple cracks in piezoelectric materials. International Journal of Solids and Structures 36, 4183–4202.

Hao T.H., Shen Z.Y., 1994. A new boundary condition of electric fracture mechanics and its applications. Engineering Fracture Mechanics 47, 793–802.

Heyliger P., 1997. Exact solutions for simply supported laminated piezoelectric plates. ASME Journal of Applied Mechanics 64, 299.

Itou S., 1978. Three dimensional waves propagation in a cracked elastic solid. ASME Journal of Applied Mechanics 45, 807–811.

Itou S., 1979. Three dimensional problem of a running crack. International Journal of Engineering Science 17, 59–71.

Lee J.S., Jiang L.Z., 1996. Exact electro-elastic analysis of piezoelectric laminate via state space aproach. International Journal of Solids and Structures 33, 977.

Li S., Mataga P.A., 1996-a. Dynamic crack propagation in piezoelectric materials-part I. Electrode solution. Journal of the Mechanics and Physics of Solids 44, 1799–1830.

Li S., Mataga P.A., 1996-b. Dynamic crack propagation in piezoelectric materials-part II. Vacuum solution. Journal of the Mechanics and Physics of Solids 44, 1831–1866.

Meguid S.A., Wang X.D., 1998. Dynamic anti-plane behaviour of interacting cracks in a piezoelectric medium. International Journal of Fracture 91, 391–403.

Morse P.M., Feshbach H., 1958. Methods of Theoretical Physics, Vol.1, McGraw-Hill, New York.

Narita K., Shindo Y., 1998-a. Anti-plane shear crack growth rate of piezoelectric ceramic body with finite width. Theoretical and Applied Fracture Mechanics 30, 127–132.

Narita K., Shindo Y., 1998-b. Scattering of Love waves by a surface-breaking crack in piezoelectric layered media. JSME International Journal, Series A 41, 40.

Narita K., Shindo Y., 1999. Scattering of anti-plane shear waves by a finite crack in piezoelectric laminates. ACTA Mechanica 134, 27–43.

Narita K., Shindo Y., Watanabe K., 1999. Anti-plane shear crack in a piezoelectric layered to dissimilar half spaces. JSME International Journal, Series A 42, 66–72.

Pak Y.E., 1990. Crack extension force in a piezoelectric material. Journal of Applied Mechanics 57, 647–653.

Pak Y.E., 1992. Linear electro-elastic fracture mechanics of piezoelectric materials. International Journal of Fracture 54, 79–100.

Park S.B., Sun C.T., 1995-a. Effect of electric field on fracture of piezoelectric ceramics. International Journal of Fracture 70, 203–216.

Park S.B., Sun C.T., 1995-b. Fracture criteria for piezoelectric ceramics. Journal of American Ceramics Society 78, 1475–1480.

Shindo Y., Domon W., Narita F., 1998. Dynamic bending of a symmetric piezoelectric laminated plate with a through crack. Theoretical and Applied Fracture Mechanics 28, 175.

Shindo Y., Narita F., Tanaka K., 1996. Electroelastic intensification near anti-plane shear crack in orthotropic piezoelectric ceramic strip. Theoretical and Applied Fracture Mechanics 25, 65–71.

Sosa H., 1992. On the fracture mechanics of piezoelectric solids. International Journal of Solids and Structures 29, 2613–2622.

Sosa H., Khutoryansky N., 1999. Transient dynamic response of piezoelectric bodies subjected to internal electric impulses. International Journal of Solids and Structures 36, 5467–5484.

Suo Z., 1993. Models for breakdown-resistant dielectric and ferroelectric ceramics. Journal of Mechanics and Physics of Solids 41, 1155–1176.

Suo Z., Kuo C.-M., Barnett D.M., Willis J.R., 1992. Fracture mechanics for piezoelectric ceramics. Journal of Mechanics and Physics of Solids 40, 739–765.

Tang Y.Y., Noor A.K., Xu K., 1996. Assessment of computational models for thermoelectroelastic multilayered plates. Computers and Structures 61, 915.

Tauchert T.R., 1996. Cylindrical bending of hybrid laminates under thermo-electro-mechanical loading. Journal of Thermal Stresses 19, 287.

Wang B., 1992. Three dimensional analysis of a flat elliptical crack in a piezoelectric materials. International Journal of Engineering Science 30 (6) 781–791.

Yu S.W., Chen Z.T., 1998. Transient response of a cracked infinite piezoelectric strip under anti-plane impact. Fatigue and Engineering Materials and Structures 21, 1381–1388.

Zhang T.Y., Tong P., 1996. Fracture mechanics for a mode III crack in a piezoelectric material. International Journal of Solids and Structures 33, 343–359.

Zhang T.Y., Qian C.F., Tong P., 1998. Linear electro-elastic analysis of a cavity or a crack in a piezoelectric material. International Journal of Solids and Structures 35, 2121–2149.

Zhou Z.G., Han J.C., Du S.Y., 1999-a. Two collinear Griffith cracks subjected to uniform tension in infinitely long strip. International Journal of Solids and Structures 36, 5597–5609.

Zhou Z.G., Han J.C., Du S.Y., 1999-b. Investigation of a Griffith crack subject to anti-plane shear by using the non-local theory. International Journal of Solids and Structures 36, 3891–3901.